

# Combustion and Kinetics Parameters Investigation of Raw and Torrefied Cocoa Pod Shells by Thermogravimetric Analysis

Untoro Budi Surono<sup>\*‡</sup>, Harwin Saptoadi<sup>\*\*</sup>, Tri Agung Rohmat<sup>\*\*</sup>

\* Doctoral Student of Mechanical and Industrial Engineering Department, Universitas Gadjah Mada, Jln. Grafika Nomor 2, Yogyakarta, Indonesia

‡ Mechanical Engineering Depart., Universitas Janabadra, Jln. T.R. Mataram Nomor 55-57, Yogyakarta, Indonesia

\*\* Mechanical and Industrial Engineering Department, Universitas Gadjah Mada, Jln. Grafika Nomor 2, Yogyakarta, Indonesia

(untorobs@janabadra.ac.id, harwins@ugm.ac.id, [triagung\\_rohmat@ugm.ac.id](mailto:triagung_rohmat@ugm.ac.id))

‡ Corresponding Author: Untoro Budi Surono, Mechanical Engineering Depart., Universitas Janabadra, Jln. T.R. Mataram Nomor 55-57, Yogyakarta, Indonesia [untorobs@janabadra.ac.id](mailto:untorobs@janabadra.ac.id)

*Received: 14.12.2021 Accepted: 06.01.2021*

**Abstract-** Torrefaction is one of the techniques to produce solid fuel from cocoa pod shells (CPS). In this research, changing combustion characteristic and kinetics of CPS after torrefaction process was investigated using Coats – Redfern Method. Torrefied CPS processed at temperatures of 200, 250, and 300°C and holding times of 0, 30, 60, and 90 min were used in this investigation. The results proved that the ignition and burnout temperatures shifted to higher value, while the peak mass loss rate tend to lower value when the torrefaction temperature and the holding time increased. The period of volatile release during the combustion process was shorter along with longer holding time and higher temperature of torrefaction. The maximum mass loss rate of raw CPS was 0.12005 g/min, while torrefied CPS has range between 0.046 to 0.114 g/min. The maximum mass loss rates of all samples decrease with increasing fuel ratio (FR). The activation energy increases gradually with increasing severity of torrefaction. The value of activation energy in the devolatilization and volatile combustion stage is greater compared to that of the char combustion stage.

**Keywords-** torrefaction, combustion characteristic, cocoa pod shells, Coats – Redfern method, activation energy

## Introduction

The using coal in Indonesia's power plants is still high because coal reserves are currently still abundant. In the future, the use of coal as power plant fuels must be reduced or replaced for two reasons, the depletion of coal reserves and the problem of environmental pollution. The Indonesian government has targeted coal reduction from 57% in 2018 to 41% in 2050 [1]. To achieve the target, biomass is a reliable material to replace coal. Indonesia has abundant biomass resources such as agricultural and forestry wastes because Indonesia is a tropical and agriculture based country [2]. Besides that, biomass is considered as one of the prospective sustainable and environmentally friendly for renewable energy resources [3]–[5]. Biomass is renewable and neutral carbon energy sources to support energy security [6]. Energy security is a vital factor for economic growth, especially in developing countries [7]. Therefore, utilization of agricultural wastes as energy source has get more attention [8], [9].

Biomass is a renewable energy source whose properties can be converted to those of coal as close as possible. Therefore biomass can be used partially in existing coal power plants, with least modifications to the handling and combustion equipment [10]. Biomass must be processed so that its characteristics are as similar as to coal. A technology that can convert the characteristics of biomass to be close to those for coal is torrefaction [11], [12].

Torrefaction is a kind of thermo-chemical method of pretreatment the biomass carried out at relatively low temperature of between 200 - 300°C where raw biomass is heated in an inert atmosphere to remove the moisture and oxygenated compounds, which aims to upgrade the fuel properties [13]–[15]. Torrefaction is a low temperature pyrolysis process run at low heating rate. The process is characterized by a low heating rate at the desired holding time (usually 10 – 60 min) [16]. Torrefaction is often referred to as temperate pyrolysis, slow pyrolysis, roasting, and thermal pretreatment, in accordance with its utilization [17]. The

biomass partially decomposes due to heat effect during torrefaction. This process results in biomass with a modified chemical components that has new properties [18]. The solid product of the process has higher energy density but lower moisture and volatile contents compared to the untreated biomass [3], [11].

Changing the biomass properties will affect the behavior of biomass combustion. Information about combustion characteristics of solid fuel, such as reaction peak, ignition, and burnout temperatures, are needed for interpretation of fuel combustion. Burning time and maximum combustion rate are also useful for fuel combustion interpretation. Combustion kinetics parameters including activation energy, pre-exponential factor, and reaction order are fundamental information to predict the combustion process. The designing, operating, and improving efficiency of combustion furnace also requires the information [19],[20]. Thermogravimetric analysis (TGA) has become a common method to estimate the combustion or pyrolysis behaviors of solid material [21],[22]. In this method, decreasing of sample mass related to increasing temperature is logged. The mass loss data generated from TGA could be utilized to identify the combustion characteristics and the combustion kinetic parameters [23]. The activation energy is a parameter to determine the lowest energy which must available so that potential reactants in a chemical system are able to react chemically [24]. The activation energy is calculated to determine the least amount of energy needed to begin a chemical reaction, whereas the pre-exponential factor can be determined by identifying the reaction mechanism [25].

Numerous researchers have interested in the using TG and DTG as functional tools to describe the combustion characteristics and kinetics of biomass, where: TG – thermogravimetry presents the change of mass loss throughout combustion under increasing temperature, DTG – the first derivative of the TG curve, illustrating the mass loss rate variation. Combustion Kinetics of some biomass was investigated using TG and DTG such as leaf stem, leaf, and date palm seed [26], pine sawdust [19], wood, olive leaves,

and pruning [27], red pepper [28], solid recovered fuel [29], miscanthus, acacia, and pine [30], tobacco waste [31], bamboo, sugarcane bagasse [32], sugarcane and cassava bagasse [33], sida [4], and karanja fruit hulls [20].

Most of previous researchers aim to compare the combustion characteristics and kinetics between several untreated biomass. Meanwhile, in-depth research on the effect of biomass pretreatment, particularly the effect of torrefaction holding time and temperature on combustion characteristics and kinetics has not been widely studied. Therefore, the main interest of this research work was to investigate the effect of torrefaction holding time and temperature on combustion characteristics of CPS. The CPS was torrefied at temperatures of 200, 250, and 300 °C and four different holding times (0, 30, 60, and 90 min), while proximate and ultimate analyses, as well as HHV, were performed for raw and torrefied CPS. In addition, burning tests were carried out to obtain ignition, peak, and burnout temperatures by using TG analysis. Calculating the activation energy and pre-exponential factor of CPS combustion process applied Coats-Redfern method.

## 2. Materials and Method

### 2.1. Sample Preparation

In the present work, raw and torrefied CPS samples were used to study the thermal kinetics under air environment. Torrefied CPS samples were obtained from torrefaction processes under combination of three temperatures (200 °C, 250 °C, 300 °C) and four holding times (0 min, 30 min, 60 min, 90 min). Raw CPS sample was obtained from a cocoa plantation in Gunung Kidul, Indonesia. Torrefaction was performed by placed the raw CPS in tubular torrefaction reactor heated by Nichrome electric heater and flowed with nitrogen as inert gas. Furthermore, each torrefied sample was weighed then wrapped in an airtight plastic bag for further analysing.

**Table 1.** Proximate analysis and HHV of CPS at various temperatures and holding times.

| Torrefaction condition |          | Proximate Analysis (wt%, adb) |          |              |      | HHV (MJ/kg) |
|------------------------|----------|-------------------------------|----------|--------------|------|-------------|
| TT (°C)                | HT (min) | Moisture                      | Volatile | Fixed carbon | Ash  |             |
|                        | Raw CPS  | 10.66                         | 60.78    | 21.74        | 6.82 | 16.35       |
| 200                    | 0        | 9.21                          | 58.26    | 22.66        | 9.86 | 17.17       |
| 200                    | 30       | 6.96                          | 58.20    | 25.89        | 8.94 | 18.31       |
| 200                    | 60       | 6.37                          | 59.01    | 25.80        | 8.80 | 18.80       |
| 200                    | 90       | 7.26                          | 58.38    | 25.60        | 8.75 | 19.00       |
| 250                    | 0        | 8.56                          | 59.36    | 23.22        | 8.85 | 17.81       |
| 250                    | 30       | 6.66                          | 57.94    | 29.13        | 6.26 | 19.58       |
| 250                    | 60       | 6.02                          | 53.08    | 33.21        | 7.67 | 21.08       |
| 250                    | 90       | 5.78                          | 54.13    | 33.18        | 6.91 | 21.20       |
| 300                    | 0        | 6.94                          | 57.42    | 27.47        | 5.52 | 20.57       |
| 300                    | 30       | 10.60                         | 41.97    | 37.76        | 4.98 | 21.68       |
| 300                    | 60       | 6.33                          | 44.77    | 39.24        | 4.92 | 21.87       |
| 300                    | 90       | 6.39                          | 41.39    | 39.11        | 4.74 | 23.11       |

### 2.2. Sample Characteristics

Prior to proximate and ultimate analyses, as well as HHV, each sample was milled and sieved into particles sized of 177–250 μm. Proximate analyses for torrefied and raw CPS were carried out twice according to ASTM 3171, 3174, and 3175 to obtain moisture, volatile matter, and fixed carbon contents. Fixed carbon and volatile matter ratio which is defined as the fuel ratio (FR) is used to represent the properties of a solid fuel [34]. A bomb calorimeter IKA C6000 was used to determine HHV of all samples. These analyzes were conducted twice for repeatability. Proximate analyses and HHV of CPS and treated samples are given in Table 1.

### 2.3. Thermogravimetric analysis

The combustion investigation was performed using a self-designed macro thermo-balance. Figure 1 illustrates the configuration of the experimental device. Each experiment used a sample of approximately 0.25 g. Then the sample was put in an alumina crucible with a thermocouple placed close to the sample to observe the temperature. The loss of the sample mass was logged from ambient temperature to 600 °C with 65 °C/min heating rate. Each test was performed at least twice to confirm that the experimental data had good repeatability. The mass loss rate of the samples was represented as a function of combustion time. The combustion characteristics, including ignition and burnout temperatures were determined from TG/DTG curve in accordance with the previous literatures [35]. The burnout temperature was determined based on the mass loss rate which was less than 1 wt.%/min. The TG/DTG curve (as shown in Figure 2) is used to determine the ignition temperature. The ignition temperature is determined based on the correlation between the highest value of the DTG profile (point A) and the

beginning of devolatilization on the TG curve. A vertical line was sketched from the peak of the DTG curve and crossed with the TG curves (point B), and then from the intersection point, a line that tangents to the TG curve was drawn. The tangent met the parallel lines of the beginning devolatilization at point C. A line was drawn through point C in a downward direction, which met the temperature curve at point D of the temperature curve. The point D was identified as the ignition temperature.

### 2.4. Kinetic Analysis

The design and optimization of combustion system requires the chemical kinetics of biomass combustion information. An integral method is one of the methods to analyze combustion kinetics using non-isothermal TG data. Combustion reactions are considered as one-dimensional diffusion process to simplify the kinetic calculations. Coats-Redfern method is the most generally method applied in the kinetic analysis of biomass thermal decomposition. Naqvi et al. [36] and Surahmanto et al. [37] determined the activation energy using the Coats-Redfern method in the kinetic analysis of paddy husk and oil palm solid wastes.

The kinetic analysis of CPS combustion was determined by Arrhenius law, which was given by the below equation

$$\frac{d\alpha}{dt} = k(T)f(\alpha) \quad (1)$$

$$\text{where } \alpha \text{ is defined as, } \alpha = (m_o - m_t)/(m_o - m_f) \quad (2)$$

$$\text{and } k(T) = A \exp(-E_a/RT) \quad (3)$$

where  $m_o$ ,  $m_t$ , and  $m_f$  are the initial mass, the mass at time  $t$ , and the final mass.  $T$  is temperature (K),  $A$  is pre-exponential factor (1/min),  $R$  is the gas constant (0.0083 kJ/mol K), and  $E$  is the activation energy (kJ/mol).

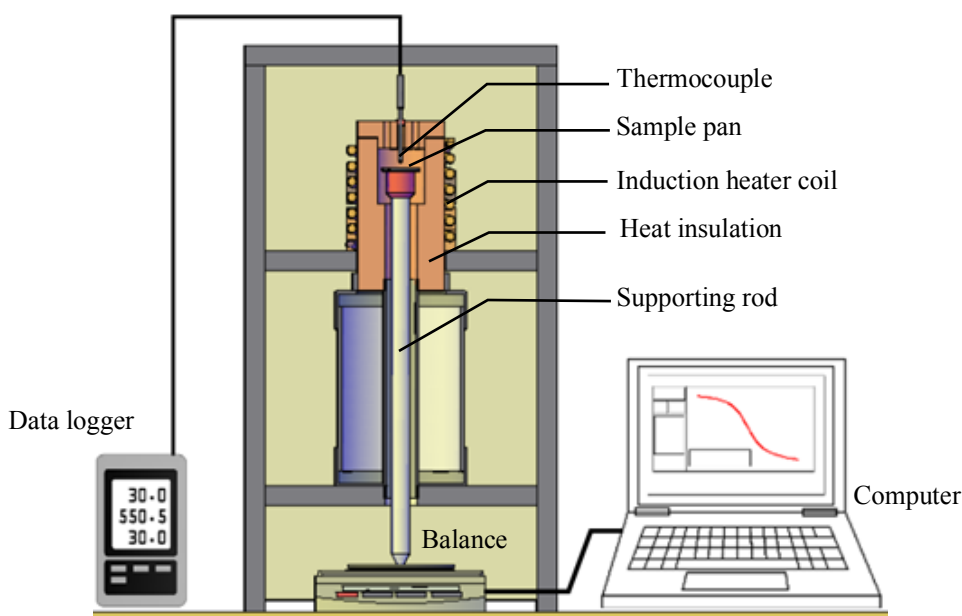


Fig. 1. The schematic of Macro-Thermobalance and instruments

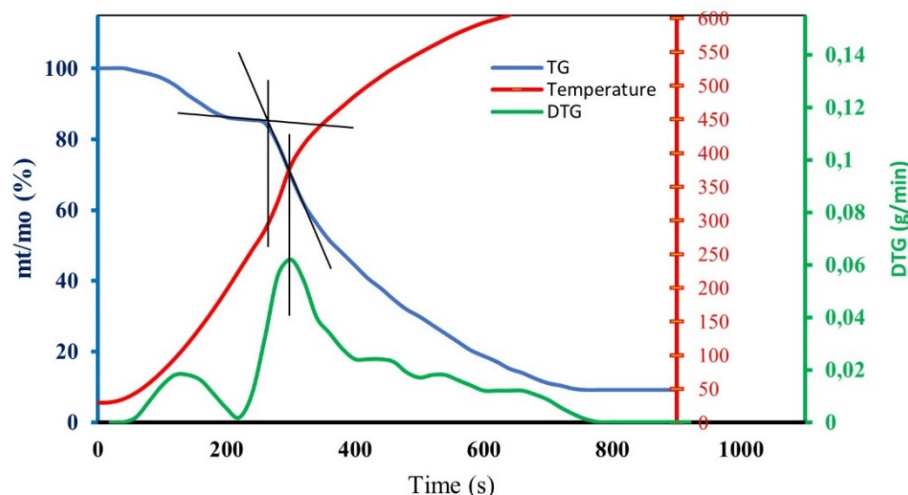


Fig. 2. Ignition temperature definition sketch

For heating rate  $\beta$  ( $^{\circ}\text{C}/\text{min}$ ) during combustion is constant value,  $\beta = dT/dt$ , Eq. (1) can be converted as below,

$$d\alpha/f(\alpha) = (k/\beta) dT \quad (4)$$

Integrating Eq. (4) gives a new equation,

$$g(\alpha) = \int_0^{\alpha} d\alpha/f(\alpha) = A/\beta \int_{T_0}^T \exp(-Ea/RT)dT \quad (5)$$

where  $g(\alpha)$  is the conversion integral function.

Eq. (5) is integrated using the Coats-Redfern model and becomes:

$$\ln \left[ \frac{g(\alpha)}{T^2} \right] = \ln \left[ \frac{AR}{\beta E} \left( 1 - \frac{2RT}{E} \right) \right] - \frac{E}{RT} \quad (6)$$

If assuming that  $2RT/E \ll 1$  than Eq. (6) becomes:

$$\ln[g(\alpha)/T^2] = \ln[AR/\beta E] - E/RT \quad (7)$$

In this work, diffusion model for Solid-State mechanism was applied. For 1-D diffusion model,  $g(\alpha)$  would be  $g(\alpha) = \alpha^2$ .

Plots of  $\ln[g(\alpha)/T^2]$  versus  $1/T$  under heating rate of  $65^{\circ}\text{C}/\text{min}$  were resulted from the torrefaction processes with different temperatures and holding times. The plot was separated into two segments, based on linearity. The slope and interception of the plot was applied to evaluate the activation energy. The correlation coefficient value ( $R^2$ ) showed the accuracy of the calculation. The combustion region was divided into two segments (removal and volatiles combustion and combustion of char), so that the kinetics can be calculated much accurately

### 3. Results and discussion

#### 3.1. Combustion characteristics of materials

Combustion characteristics of solid matter can be determined quickly by thermogravimetric analysis (TGA). Samples of torrefied CPS were subjected to thermal analysis

to recognize the effect of holding time and torrefaction temperature on the combustion characteristic of CPS. The results of this study were shown in the form of TG and DTG curves. TG and DTG profiles make them possible to identify the mass loss which occur throughout the combustion process. Figure 3 presents TG and DTG profiles with center of attention on the thermal behavior of torrefied CPS.

The biomass combustion is typically divided in three stages, i.e. loss of moisture, devolatilization and combustion of volatile, and char combustion [38][39]. The decreasing sample mass took place due to the removal of moisture content along with the gradual increasing the furnace temperature. The releasing and burning volatile matter occurred after removal of moisture content. In the second stage, the acceleration of mass loss rate leads to the TG curve that gets sharper and reaches the peak at a certain temperature. The combustion of char was depicted by a trend of the TG curve which downward slowly along with rising the furnace temperature. Finally, its mass loss will stop to decrease caused by complete combustion.

##### 3.1.1. Mass loss of the samples

The samples mass loss at the first stage initiated from the furnace temperature  $50^{\circ}\text{C}$  to  $190^{\circ}\text{C}$  was due to releasing moisture content, which was about 12 - 15 wt.%. The second stage started from  $190^{\circ}\text{C}$  to around  $300^{\circ}\text{C}$  was due to removal of the volatile matters and oxidation. The TG curve became steeper because of the accelerating the mass loss rate and reached the peak at a specific temperature. After the volatiles was removed from the samples, the combustion process was continued by oxidation of the char until the mass of the sample was not decrease anymore. The TG curve in the stage sloped slightly and more stable compared to the second stage. Figure 3 also showed that the longer the holding time and the higher the temperature, the shorter the volatile decomposition stage period.

The main characteristic of CPS combustion was that the mass loss rate in the third stage was notably lower than that in the second stage as shown in Fig. 3. Fang et al. [40] also

obtained the same result about this phenomenon in some biomass samples. It was caused by the volatile content that was higher than that of the fixed carbon content. The fixed carbon can ignite and then burn at higher temperatures than that of the volatile matter. The TGA curve of torrefied CPS at 200 °C was slightly different from each other as shown in Figure 3.a. These results indicate that in light torrefaction, the effect of holding time variation is not significant. Whereas for torrefied 250 °C, the TGA curve showed a clear difference except for holding time of 60 min and 90 min where the curves are almost coincided. It means that the effect of increasing a

holding time of more than 60 min is no longer significant. The TGA curve of torrefied 300 °C with various holding times showed differently. The fact indicates that difference in holding times has a significant effect on the TGA curve at severe torrefaction. Combustion residue in the form of ash could also be observed from the DTG curve. The longer the holding time and the higher the torrefaction temperature, the more the combustion residue. TGA curves also illustrate that the longer the holding time and the higher the torrefaction temperature, the second stage took place in a shorter period.

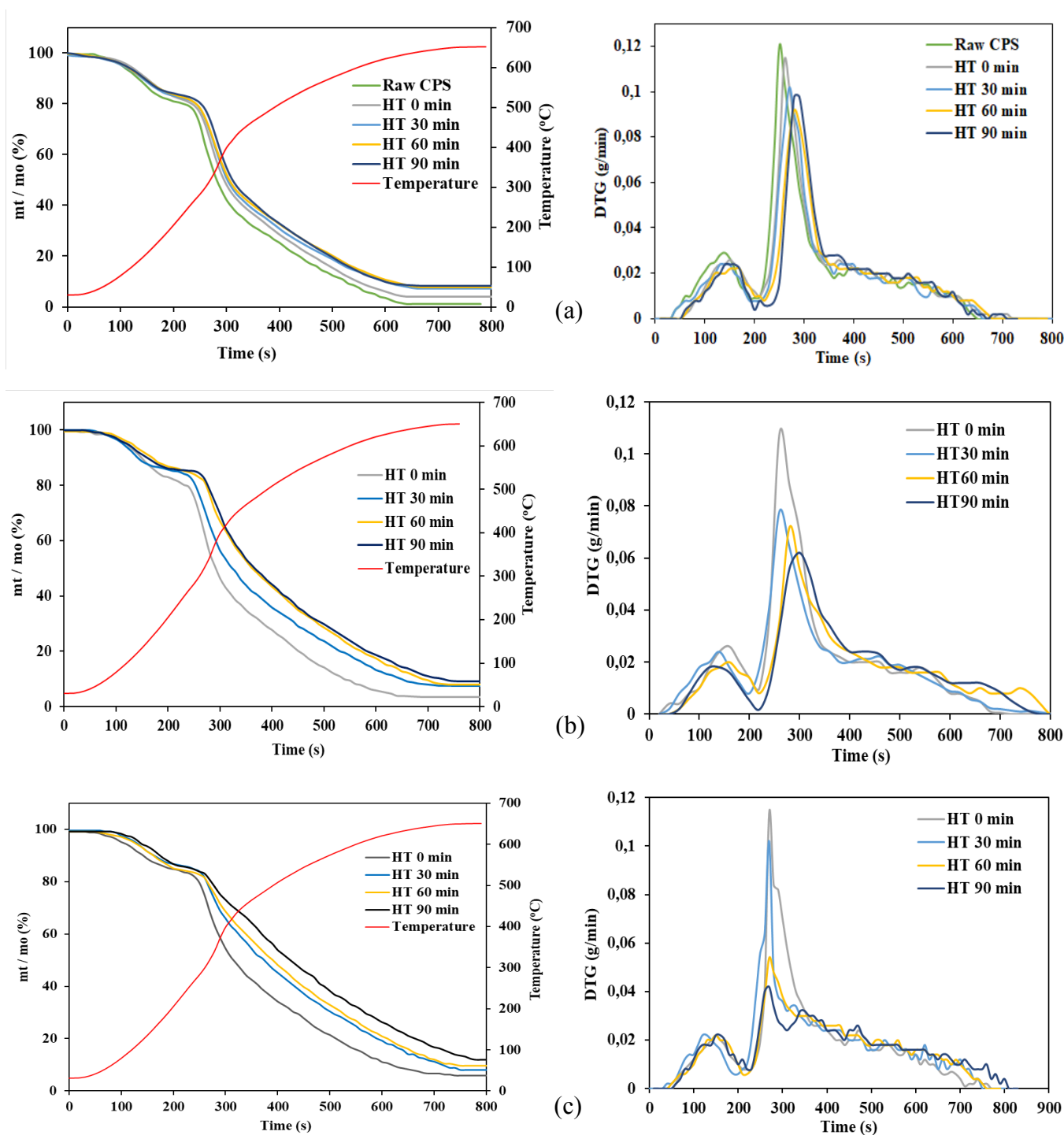


**Fig. 3.** Comparison TG/DTG curves of torrefied CPS at different torrefaction temperatures: a) 200 °C, b) 250 °C, and c) 300 °C



### 3.1.2. Mass loss rate

The DTG curve exhibits mass loss rate of the sample. From the DTG curve in Fig. 3, it is recognized that there are two peaks of the mass loss rate. The first peak relates to the releasing moisture and the second peak corresponds to devolatilization. The first peak occurs around 150 seconds which corresponds to a temperature of 135 °C. The second peak relates to the devolatilization and combustion of volatile matter processes. The second peak of the samples is different from each other. The maximum mass loss rate of raw CPS was 0.12005 g/min, while torrefied CPS has range between 0.046 to 0.114 g/min, which depend on the holding time and the torrefaction temperature of the torrefaction process. The maximum mass loss rate decreased from 0.114 g/min for torrefied at 200 °C and 0 min to 0.046 g/min for torrefied at 300 °C and 90 min. Table 2 reveals that the second peak temperature of CPS was lower than torrefied CPS. Torrefied CPS at 200 °C and 0 min holding time has the lower second peak temperature (299.4 °C) of treated CPS, while the highest second peak temperature (398.8 °C) was achieved by torrefied CPS at 250 °C and 90 min holding time. The summit of mass loss rate and temperature can be used to evaluate the reactivity of the sample. The higher the maximum mass loss rate and the lower the peak temperature, the higher the sample reactivity. Liu et al. [41] confirmed that the torrefaction increased the peak temperature and decreased the summit of mass loss rate. This phenomenon indicated that reactivity of bamboo decreased due to torrefaction process.

### 3.1.3. Fuel Ratio analysis

Figure 4 shows the relationships between Fuel Ratio (FR) and the summit of mass loss rate and illustrated that the cause of the difference in the maximum mass loss rate was due to the torrefaction process. The value of FR rose with increasing torrefaction severity was due to increasing fixed carbon and decreasing volatile matter. In the previous research that carried out by Park et al., the value of FR is in the range of 0.244 - 1.245, 0.435 - 3.443, and 0.070 - 4.345 for rice husk, wood chip, and wood pellet that pyrolyzed at 300, 400, and 500 °C [34]. In the present work, the FR was in the range of 0.358 for raw CPS to 0.945 for torrefied CPS at 300 °C and 90 min. The increasing FR was more significant at the holding time of 90 min than the others. As shown in Fig. 3, the FR and the maximum mass loss rate had opposing trends. With increasing the FR, maximum mass loss rate decreased. The FR and the maximum mass loss rate were correlated with the power model,  $y = 5394 x^{-0.249}$ , where y was the maximum mass loss rate and x was FR. The model obtained had a high correlation which was indicated by an R<sup>2</sup> value of more than 0.95 and was valid for FR from 0.358 to 0.945.

### 3.1.4. Ignition and burnout temperatures

One of the crucial combustion characteristics of fuel is ignition temperature. The ignition temperature indicates how easily or difficultly fuel gets ignited. The lower the ignition temperature, the easier the fuel ignites. As pointed out in Table 2, the ignition temperature of CPS and torrefied CPS is in the range of 263 to 302 °C depends on the holding time and

torrefaction temperature. The ignition temperature of CPS was 263 °C. It is higher than ignition temperature of wheat straw (243 °C) and rape straw (247 °C) but lower than flax straw (266 °C) [42]. For torrefied CPS at 200 °C and 250 °C, the ignition temperatures were 265 to 285 °C and 265 to 300 °C, respectively, while for torrefied CPS at 300 °C, the ignition temperatures were 268 to 302 °C. Generally, the longer the holding time and the higher the torrefaction temperature, the ignition temperature shifted to higher. It can be caused by the amount of component in biomass that is easy to burn released during torrefaction process.

The burnout temperature of CPS is 636.4 °C, whereas torrefied CPS is between 640.6 and 651.2 °C as presented in Table 2. Similar to the ignition temperatures, the burnout temperature tent to increase along with increasing the holding time and the torrefaction temperature. The higher the burnout temperature indicates the more the time for fuels to burn out caused by the lower the volatile content and the higher the fixed carbon content.

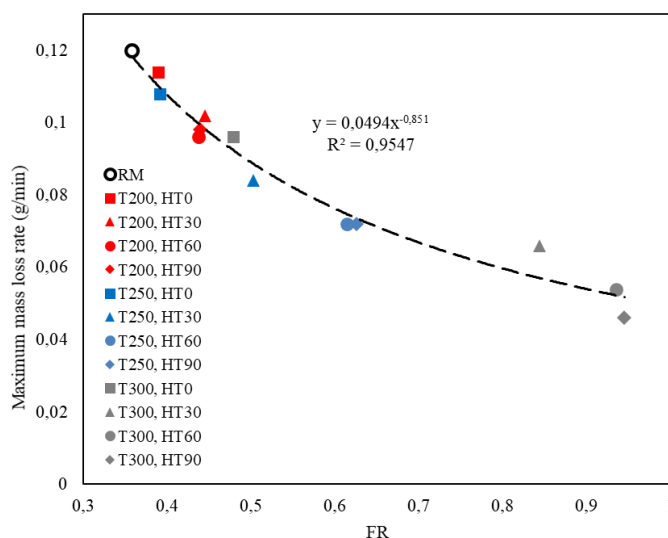


Fig. 4. Correlation of FR and maximum mass loss rate

Table 2. Combustion characteristics of torrefied CPS

| Torrefaction condition |          | Temperature (°C) |                      |         |
|------------------------|----------|------------------|----------------------|---------|
| TT (°C)                | HT (min) | Ignition         | 2 <sup>nd</sup> peak | burnout |
| RM                     |          | 263              | 282.7                | 636.4   |
| 200                    | 0        | 265              | 299.4                | 640.6   |
| 200                    | 30       | 268              | 319.7                | 646.8   |
| 200                    | 60       | 270              | 373.6                | 649.9   |
| 200                    | 90       | 285              | 373.6                | 650.6   |
| 250                    | 0        | 265              | 299.4                | 643.6   |
| 250                    | 30       | 270              | 299.4                | 648.4   |
| 250                    | 60       | 287              | 343.5                | 650.2   |
| 250                    | 90       | 300              | 398.8                | 650.8   |
| 300                    | 0        | 268              | 299.4                | 649.6   |
| 300                    | 30       | 283              | 319.7                | 650.4   |
| 300                    | 60       | 298              | 343.5                | 650.4   |
| 300                    | 90       | 302              | 319.7                | 651.2   |

3.2. Combustion kinetics

The kinetic parameters were determined evaluating the TGA data applying the Coats-Redfern method. Figure 5 shows the examples of the plotting  $\ln [g(\alpha)/T^2]$  against  $1/T$  of the Coats-Redfern method. Table 3 presents the calculation results of activation energy (E) and pre-exponential factor (A) of the torrefied samples. Activation energy and pre-exponential factor are obtained from slopes of straight lines by using Eq. (7). Most of the correlation coefficients were above 0.99 denoting the reliability of the calculations. The difference in behavior can be described by comparing the range of activation energy of each combustion stage with the different torrefaction temperatures and holding times.

Torrefaction has effects on the kinetic parameters of the CPS. In Table 3, the activation energy and pre-exponential factor increase with increasing of torrefaction severity. The phenomena are due to the increasing number of compounds with weak chemical bonds that are released when the torrefaction temperature is higher, and the holding time of torrefaction is longer. As listed in Table 3, the lowest value of activation energy of torrefied CPS was 30.146 kJ/mol in the second stage and 15.114 kJ/mol in the third stage of torrefaction at 200 °C, 0 min holding time. While the higher value of activation energy of torrefied CPS was 36.087 kJ/mol in the second stage and 28.276 kJ/mol in the third stage of torrefaction at 300 °C.

The values of activation energy and pre-exponential factor in the second stage of combustion which is the devolatilization stage are greater compared to those of char combustion stage. The activation energies are in the range of 32.690 to 36.087 kJ/mol in the second stage, and these are 15.114 – 28.276 kJ/mol in the third stage. The pre-exponential factor for the torrefied samples were 25.1 – 67.6 min<sup>-1</sup> in the second stage and 1.02 - 8.87 min<sup>-1</sup> in the third stage. In the second stage, releasing volatile content takes place in low temperature conditions, in which molecules are slow down, and energy requirement for molecules activation is higher. Also, the devolatilization reaction in the second stage creates a permeable char structure, which results favorable conditions

for oxygen diffusion to the surface and lead to less activation energies requirement in the third stage. It shows that activation energy in high temperature range is lower than that in low temperature range [23].

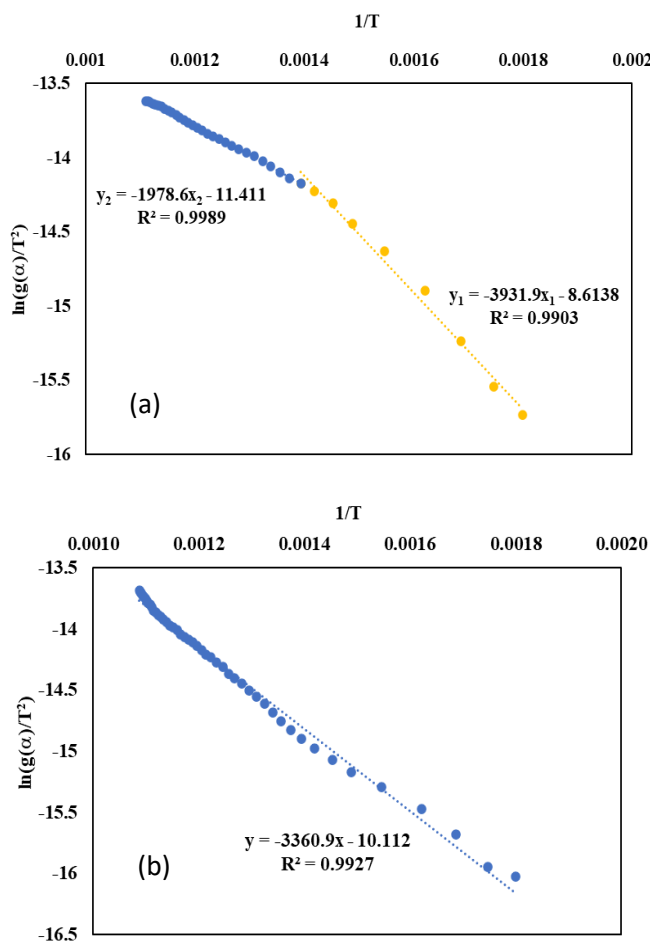


Fig. 5. Linear regression curves by plotting  $\ln (g(\alpha)/T^2)$  versus  $1/T$  a) torrefied CPS at 200°C, 90 min holding time; b) torrefied CPS at 300°C, 60 min holding time.

Table 3. Activation energy (E) and pre-exponential factor (A) of torrefied CPS

| Torrefaction condition |          | Second stage |           |                    | Third stage |           |                    |
|------------------------|----------|--------------|-----------|--------------------|-------------|-----------|--------------------|
| TT (°C)                | HT (min) | E (kJ/mol)   | A (1/min) | R <sup>2</sup> (%) | E (kJ/mol)  | A (1/min) | R <sup>2</sup> (%) |
| 200                    | 0        | 30.146       | 25.1      | 98.01              | 15.114      | 1.02      | 98.99              |
| 200                    | 30       | 31.644       | 34.1      | 97.89              | 15.139      | 1.03      | 99.79              |
| 200                    | 60       | 32.231       | 37.6      | 99.20              | 16.161      | 1.28      | 98.36              |
| 200                    | 90       | 32.690       | 46.4      | 99.03              | 18,128      | 1.57      | 99,89              |
| 250                    | 0        | 31.347       | 39.6      | 96.10              | 15.619      | 1.20      | 99.61              |
| 250                    | 30       | 31.722       | 35.9      | 97.20              | 17.643      | 1.55      | 98.57              |
| 250                    | 60       | 32.290       | 22.9      | 99.05              | 25.789      | 6.59      | 99.82              |
| 250                    | 90       | 33.978       | 52.0      | 99.63              | 25.852      | 6.67      | 99.66              |
| 300                    | 0        | 33.930       | 38.3      | 97.58              | 21.133      | 3.04      | 99.74              |
| 300                    | 30       | 36.087       | 67.6      | 97.64              | 27.466      | 8.48      | 99.57              |
| 300                    | 60       | -            | -         | -                  | 27.943      | 8.87      | 99.27              |
| 300                    | 90       | -            | -         | -                  | 28.276      | 8,64      | 96.50              |

#### 4. Conclusions

The results of TGA for torrefied CPS are provided in this study. The torrefaction process at longer holding times and higher temperatures contributed to the increase of ignition and burnout temperatures, while the maximum mass loss rate tended to decrease. The shorter period of devolatilization took place along with longer holding times and higher temperatures. The activation energy and pre-exponential factor of the biomass combustion are determined using the Coats-Redfern method. The activation energies in the devolatilization stage are 32.690 – 36.087kJ/mol, and in the char combustion stage are 15.114 – 28.276kJ/mol. The activation energy increases gradually with increasing the torrefaction severity. The values of activation energy and pre-exponential factor in the devolatilization stage are greater compared to those in the char combustion stage.

#### Acknowledgements

The authors would like to acknowledge to The Indonesia Endowment Fund for Education for financial supports on this research.

#### References

- [1] SGNEC, Indonesia Energy Outlook (IEO) 2019, Secretary General of the National Energy Council, 2019.
- [2] O. T. Winarno, Y. Alwendra, and S. Mujiyanto, "Policies and strategies for renewable energy development in Indonesia," 5th International Conference on Renewable Energy Research and Applications (ICRERA), Birmingham, pp. 270–272, 20 - 23 November 2016
- [3] A. N. Awang, A. R. Mohamed, N. Hasyierah, M. Salleh, P. Y. Hoo, and N. N. Kasim, "Torrefaction of *Leucaena Leucocephala* under isothermal conditions using the Coats – Redfern method: kinetics and surface morphological analysis," *React. Kinet. Mech. Catal.*, vol. 128, no. 2, pp. 663–680, 2019.
- [4] Z. B. Laouge and H. Merdun, "Pyrolysis and combustion kinetics of *Sida cordifolia* L. using thermogravimetric analysis," *Bioresour. Technol.*, vol. 299, p. 122602, 2020.
- [5] M. Obaidullah, S. Bram, V. K. Verma, and J. De Ruyck, "A review on particle emissions from small scale biomass combustion," *Int. J. Renew. Energy Res.*, vol. 2, no. 1, pp. 147–159, 2012.
- [6] O. Nakagoe, Y. Furukawa, S. Tanabe, Y. Sugai, and R. Narikiyo, "Hydrogen production from steam reforming of woody biomass with cobalt catalyst," 1st International Conference on Renewable Energy Research and Applications (ICRERA), pp. 2–5, 2012
- [7] L. J. R. Nunes, J. C. O. Matias, and J. P. S. Catalao, "Application of biomass for the production of energy in the Portuguese textile industry," 2nd International Conference on Renewable Energy Research and Applications (ICRERA), Madrid, pp. 336–341, 20 - 23 October 2013.
- [8] I. Carlucci, G. Mutani, and M. Martino, "Assessment of potential energy producible from agricultural biomass in the municipalities of the Novara plain," 4th International Conference on Renewable Energy Research and Applications (ICRERA), Palermo, pp. 1394–1398, 22 - 25 November 2015.
- [9] Y. Tosun, "Forestry Biomass Waste Co-Incineration in Stoker and Subsequent Solar Panel ( CSP ) ORC Station," 4th International Conference on Renewable Energy Research and Applications (ICRERA), Palermo, pp. 583–589, 22 -25 November 2015.
- [10] B. Neminda, S. Gan, C. Eastwick, and H. Kiat, "Biomass as an energy source in coal co- fi ring and its feasibility enhancement via pre-treatment techniques," *Fuel Process. Technol.*, vol. 159, pp. 287–305, 2017.
- [11] E. M. Gucho, K. Shahzad, E. A. Bramer, and N. A. Akhtar, "Experimental Study on Dry Torrefaction of Beech Wood," *Energies*, vol. 8, pp. 3903–3923, 2015.
- [12] D. A. Granados, R. A. Ruiz, L. Y. Vega, and F. Chejne, "Study of reactivity reduction in sugarcane bagasse as consequence of a torrefaction process," *Energy*, vol. 139, pp. 818–827, 2017.
- [13] J. Wannapeera, B. Fungtamman, and N. Worasuwannarak, "Effects of temperature and holding time during torrefaction on the pyrolysis behaviors of woody biomass," *J. Anal. Appl. Pyrolysis*, vol. 92, no. 1, pp. 99–105, 2011.
- [14] W. H. Chen, H. C. Hsu, K. M. Lu, W. J. Lee, and T. C. Lin, "Thermal pretreatment of wood (*Lauan*) block by torrefaction and its influence on the properties of the biomass," *Energy*, vol. 36, no. 5, pp. 3012–3021, 2011.
- [15] S. S. Thanapal, K. Annamalai, R. J. Ansley, and D. Ranjan, "Co-firing carbon dioxide-torrefied woody biomass with coal on emission characteristics," *Biomass Convers. Biorefinery*, vol. 6, no. 1, pp. 91–104, 2016.
- [16] M.U. Garba, S.U. Gambo, U. Musa, K. Tauheed, M. Alhassan, and O.D. Adeniyi, "Impact of torrefaction on fuel property of tropical biomass feedstocks," *Biofuels*, pp. 1–9, 2017.
- [17] A. Toptas, Y. Yildirim, G. Duman, and J. Yanik, "Bioresource Technology Combustion behavior of different kinds of torrefied biomass and their blends with lignite," *Bioresour. Technol.*, vol. 177, pp. 328–336, 2015.
- [18] B. Colin, J. Dirion, P. Arlabosse, and S. Salvador, "Quantification of the torrefaction effects on the grindability and the hygroscopicity of wood chips," *Fuel*, vol. 197, pp. 232–239, 2017.
- [19] J. Zhao, S. Niu, Y. Li, K. Han, and C. Lu, "Thermogravimetric Analysis and Kinetics of Combustion of Raw and Torrefied Pine Sawdust," *J. Chem. Eng. Japan*, vol. 48, no. 4, pp. 320–325, 2015.
- [20] A. Islam, M. Auta, G. Kabir, and B. H. Hameed, "A thermogravimetric analysis of the combustion kinetics of karanja ( *Pongamia pinnata* ) fruit hulls char," *Bioresour.*



- Technol., vol. 200, pp. 335–341, 2016 .
- [21] S. Ceylan, “Kinetic analysis on the non-isothermal degradation of plum stone waste by thermogravimetric analysis and integral Master-Plots method,” *Waste Manag. Res.*, vol. 33, no. 4, pp. 345–352, 2015.
- [22] X. Xing, F. Fan, S. Shi, Y. Xing, Y.X. Zhang, and J. Yang, “Fuel properties and combustion kinetics of hydrochar prepared by hydrothermal carbonization of bamboo,” *Bioresour. Technol.*, vol. 11, no. 4, pp. 9190–9204, Apr. 2016.
- [23] G. Wang, J. Zhang, J. Shao, Z. Liu, G. Zhang, T. Xu, J. Guo, H. Wang, R. Xu, and H. Lin, “Thermal behavior and kinetic analysis of co-combustion of waste biomass / low rank coal blends,” *Energy Convers. Manag.*, vol. 124, pp. 414–426, 2016.
- [24] Z. Zhao and P. Liu, “Combustion characteristics and kinetics of five tropic oilgal strains using thermogravimetric analysis,” *J. Therm. Anal. Calorim.*, 2017.
- [25] P. Parthasarathy, K. S. Narayanan, and L. Arockiam, “Study on kinetic parameters of different biomass samples using thermo-gravimetric analysis,” *Biomass and Bioenergy*, vol. 58, pp. 58–66, 2013.
- [26] H. H. Sait, A. Hussain, A. Adam, and F. Nasir, “Pyrolysis and combustion kinetics of date palm biomass using thermogravimetric analysis,” *Bioresour. Technol.*, vol. 118, pp. 382–389, 2012.
- [27] A. Garcia-maraver, J. A. Perez-jimenez, and F. Serrano-bernardo, “Determination and comparison of combustion kinetics parameters of agricultural biomass from olive trees,” *Renew. Energy*, vol. 83, pp. 897–904, 2015.
- [28] A. Alves, D. Maia, and L. C. De Morais, “Kinetic parameters of red pepper waste as biomass to solid biofuel,” *Bioresour. Technol.*, vol. 204, pp. 157–163, 2016.
- [29] T. Szucs, P. Szentannai, I. Miklos Szilagyi, and L. P. Bakos, “Comparing different reaction models for combustion kinetics of solid recovered fuel,” *J. Therm. Anal. Calorim.*, 2019.
- [30] M. Wilk, A. Magdziarz, M. Gajek, M. Zajemska, and K. Jayaraman, “Combustion and kinetic parameters estimation of torrefied pine , acacia and *Miscanthus giganteus* using experimental and modelling techniques,” *Bioresour. Technol.*, vol. 243, pp. 304–314, 2017.
- [31] W. Wu, Y. Mei, L. Zhang, R. Liu, and J. Cai, “Kinetics and reaction chemistry of pyrolysis and combustion of tobacco waste,” *Fuel*, vol. 156, pp. 71–80, 2015.
- [32] J. J. Lu and W. H. Chen, “Investigation on the ignition and burnout temperatures of bamboo and sugarcane bagasse by thermogravimetric analysis,” *Appl. Energy*, vol. 160, no. 2015, pp. 49–57, 2015.
- [33] E. R. Zanatta, T. O. Reinehr, J. A. Awadallak, S. J. Kleinubing, J. B. O. dos Santos, R. A. Bariccatti, P. A. Arroyo, and E. A. da Silva, “Kinetic studies of thermal decomposition of sugarcane bagasse and cassava bagasse,” *J. Therm. Anal. Calorim.*, vol. 125, no. 1, pp. 437–445, 2016.
- [34] S. W. Park and C. H. Jang, “Effects of pyrolysis temperature on changes in fuel characteristics of biomass char,” *Energy*, vol. 39, no. 1, pp. 187–195, 2012.
- [35] M. Liu, J. Liu, Y. Yu, Z. Wang, J. Zhou, and K. Cen, “Investigation of lignite combustion characteristics with thermal analysis,” *Adv. Mater. Res.*, vol. 614–615, pp. 25–30, 2013.
- [36] S. R. Naqvi, Y. Uemura, N. Osman, and S. Yusup, “Kinetic study of the catalytic pyrolysis of paddy husk by use of thermogravimetric data and the Coats – Redfern model,” *Res. Chem. Intermed.*, vol. 41, pp. 9743–9755, 2015.
- [37] F. Surahmanto, H. Saptoadi, H. Sulistyono, and T. A. Rohmat, “Investigation of the pyrolysis characteristics and kinetics of oil-palm solid waste by using Coats – Redfern method,” *Energy Explor. Exploit.*, vol. 38, no. 1, pp. 298–309, 2020.
- [38] H. Ullah, G. Liu, B. Yousaf, M. Ubaid, and Q. Abbas, “Bioresource Technology Combustion characteristics and retention-emission of selenium during co- fi ring of torre fi ed biomass and its blends with high ash coal,” *Bioresour. Technol.*, vol. 245, no. August, pp. 73–80, 2017.
- [39] A. Álvarez, C. Pizarro, R. García, J. L. Bueno, and A. G. Lavín, “Determination of kinetic parameters for biomass combustion,” *Bioresour. Technol.*, vol. 216, pp. 36–43, 2016.
- [40] X. Fang, L. O. Jia, and L. Yin, “A weighted average global process model based on two-stage kinetic scheme for biomass combustion,” *Biomass and Bioenergy*, vol. 48, pp. 43–50, 2013.
- [41] Z. Liu, W. Hu, Z. Jiang, B. Mi, and B. Fei, “Investigating combustion behaviors of bamboo , torre fi ed bamboo , coal and their respective blends by thermogravimetric analysis,” *Renew. Energy*, vol. 87, pp. 346–352, 2016.
- [42] I. Jiricek, P. Rudasova, and T. Zemlov, “A Thermogravimetric Study of the Behaviour of Biomass Blends During Combustion,” *Acta Polytech.*, vol. 52, no. 3, pp. 39–42, 2012.